Available online at www.sciencedirect.com
SCIENCE DIRECT®
Journal of Molecular Catalysis A: Chemical 242 (2005) 91–104
JOURNAL OF MOLECULAR CATALYSIS A: CHEMICAL
www.elsevier.com/locate/molcata

A combined experimental—molecular modeling approach for ethene–propene copolymerization with C_2-symmetric metallocenes

Nic Friederichs [a], Bing Wang [a], Peter H.M. Budzelaar [b], Betty B. Coussens [c,*]

[a] *SABIC-Europe, R&D, Department Chemistry and Catalysis, P.O. Box 319, 6160 AH Geleen, The Netherlands*
[b] *Metal-Organic Chemistry, University of Nijmegen, The Netherlands*
[c] *DSM Research BV IC-CT, P.O. Box 18, 6160 MD Geleen, The Netherlands*

Received 25 November 2004; received in revised form 30 June 2005; accepted 30 June 2005
Available online 6 September 2005

Abstract

The relation between the structural features of C_2-symmetric zirconocenes and their performance in ethene/propene (E/P) copolymerization has been investigated using a combined experimental and quantum mechanical approach. The following ligands have been studied: $(CH_3)_2Si(Indenyl)_2$; $(CH_3)_2Si(benz[e]indenyl)_2$; $(CH_3)_2Si(4\text{-phenyl-indenyl})_2$ and their 2-methyl substituted variants. Describing trends in molecular weights for ethene/propene copolymerization, using calculated relative free energies of activation for monomer insertion and chain transfer to monomer, does not work. The results suggest that this may be due to ethene propagation being limited by a step different from the insertion itself. Besides other possible hypotheses, in particular counterion effects, we have shown that a larger energy barrier may be associated with chain rotation. Combination of experimental r_2 values with calculated barriers for propene propagation and chain transfer to both monomers works much better, presumably because the anomalies associated with ethene insertion are concentrated in this experimental r_2 value. The fair agreement achieved for this mixed description method indicates that for the other reactions the rate-limiting steps are "normal". For propene homopolymerization, our results indicate that slowing down the propagation after 2,1-insertion can be important, and show that studies of copolymerization can yield valuable information about homopolymerization. Preparing high molecular weight copolymers appears to require catalyst modifications displaying a more balanced ratio of propagation and termination.

Keywords: Ethene–propene copolymerization; Homopolymerization; Metallocenes

1. Introduction

Single-site catalysts find more and more application in industrial polyolefin production. One of the legitimate strategies for replacing conventional heterogeneous catalysts with single site catalysts can be the production of polyolefins displaying a certain kind of specialty character, i.e. having an added value compared to the generally encountered polyolefins which cannot be achieved via traditional catalysis. A well-known distinguishing feature of single site catalysts is their ability to copolymerize ethene and α-olefins in a homogeneous fashion, contrary to the conventional heterogeneous Ziegler catalysts, which result in more heterogeneous copolymers. In line with this, the penetration of single site catalysts so far is mainly in the area of ethene/α-olefin copolymers like LLDPE, plastomers, elastomers and EPDM, whereas in the field of homopolymers like polyethene and especially polypropene this penetration is slower [1]. One area where single site catalysts might create an added value for large volume isotactic polypropene (iPP) is in "iPP random copolymers" and/or in so called "impact-iPP". Whereas the former is a copolymer of propene and about 5 mass percent ethene, the latter is basically a blend of iPP and an elastomer like ethene/propene rubber (EPR). The EPR serves to improve the impact properties of iPP. This impact-iPP can be produced via off-line blending

* Corresponding author. Tel.: +31 4647 60117; fax: +31 4647 60508.
E-mail addresses: nicolaas.friederichs@sabic-europe.com (N. Friederichs), bing.wang@sabic-europe.com (B. Wang), budz@sci.kun.nl (P.H.M. Budzelaar), betty.coussens@dsm.com (B.B. Coussens).

1381-1169/$ – see front matter © 2005 Elsevier B.V. All rights reserved.
doi:10.1016/j.molcata.2005.06.066

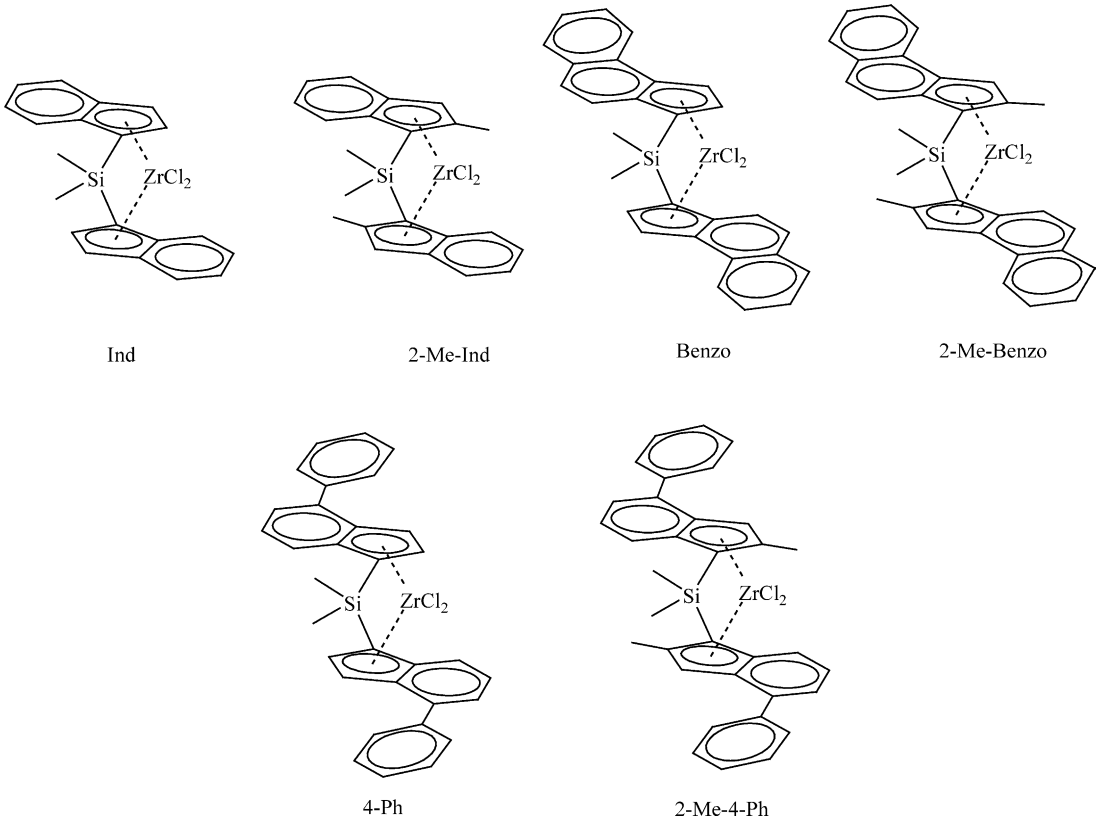

Fig. 1. Catalysts under consideration. *rac*-$SiMe_2$-bis-(1-indenyl)zirconiumdichloride (Ind), *rac*-$SiMe_2$-bis-(1-(2-methyl-indenyl))zirconiumdichloride (2-Me-Ind), *rac*-$SiMe_2$-bis-(1-(4,5-benz-[e]-Indenyl))zirconiumdichloride (Benzo), *rac*-$SiMe_2$-bis-(1-(2-methyl-(4,5-benz-[e]-indenyl))zirconiumdichloride (2-Me-Benzo), *rac*-$SiMe_2$-bis-(1-(4-phenyl-indenyl))zirconiumdichloride (4-Ph), *rac*-$SiMe_2$-bis-(1-(2-methyl-(4-phenyl-indenyl))zirconiumdichloride (2-Me-4-Ph).

of iPP and EPR, which requires an additional extrusion step. Another approach is to produce this product via a two-stage polymerization process, either in batch or via two reactors in series. In the first stage (or reactor) iPP is produced; subsequently EPR is produced by the same catalyst in the second stage (or reactor). This procedure eliminates the additional extrusion step. However, it requires a catalyst that not only meets the demands of stereo- and regioregular propene polymerization to produce high quality iPP, but also displays the capability to produce high molecular weight EPR. The impact properties of metallocene-based iPP are claimed to be superior to those of conventional Ziegler-Natta based systems [2].

The latest generation C_2-symmetric metallocenes are able to produce iPP with a crystallinity or melting point that comes close to that of conventional iPP [3,4], but unfortunately these catalysts often display a severe decrease in molecular weight upon going from propene homopolymerization to ethene-propene copolymerization. Recent publications by other groups point out that this behavior can be attributed to termination of chain growth due to chain transfer to ethene [5]. Due to this decrease in molecular weight most of the currently available metallocenes are not suited for the commercial production of impact-iPP polymers.

In order to learn more about the relation between structural features of C_2-symmetric metallocenes and their performance in ethene/propene (E/P) copolymerization (in particular the resulting molecular weights), we performed a combined experimental/molecular modeling study on a series of 6 well-known metallocenes of the Brintzinger/Spaleck type (see Fig. 1).

2. Experimental details

2.1. Catalyst components

MAO (EURECEN AL 5100/10T 10% in toluene) was obtained from Crompton and used as received. The catalysts were prepared according to standard literature procedures [3,4,6]. The purity was determined via ^{1}H NMR and was in all cases higher than 95%. The meso content was in all cases lower than 1%.

2.2. Purification of solvents and monomers

Ethene and nitrogen were purified over deoxocatalyst (BTS catalyst BASF AG) and 4A molecular sieves. Propene was purified over deoxocatalyst and 13X molecular sieves. Heptane was purified by degassing with nitrogen and subsequently over 13X molecular sieves. Toluene was distilled from sodium/benzophenone prior to use.

2.3. Ethene–propene copolymerization

Polymerizations were carried out in a stainless steel autoclave. The autoclave had an internal volume of 2 L and for these experiments the reactor was equipped with baffles and two interMIG stirrers, operated at 1400 rpm.

Five hundred millilitres of heptanes were dosed into the autoclave. A mixture of propene (typically 400 Nl/h) and ethene (typically 200 Nl/h) was dosed via separate Brooks Mass flow controllers into the headspace and the reactor pressure was set at 5 bar (abs). Off-gas was continuously vented. The temperature was set at 50 °C. Subsequently, the MAO was dosed together with an additional 350 mL of heptanes. After stirring the contents of the reactor for 30 min at 50 °C, a solution of the catalyst in approximately 1 mL of toluene was mixed with 50 mL of heptanes and subsequently pumped into the reactor and the catalyst feeding section was flushed with additional heptanes. After dosing the catalyst components, the total volume of added heptanes was 1 L. The reactor temperature was kept at 50 ± 1 °C by cooling with an oil system. After 30 min, the mixture was drawn off via a bottom valve. A mixture of isopropanol and Irganox 1076 was added.

The complete polymer solution was put in a stove and dried to constant weight at 50 °C.

To minimize mass transport limitations, the amount of catalyst was adjusted to obtain between 5 and 10 g of copolymer under the above conditions. This required 15–100 nmol, depending on the catalyst used.

Each catalyst was tested at several ratios of propene to ethene. The calculated monomer concentrations corresponding to the feed compositions (gaseous feed into the headspace of the reactor) are given as supplementary information (Supplementary data, Table S1).

2.4. GPC measurements

M_n and M_w were determined by SEC-DV. Because we are primarily interested in the degree of polymerization (P_n), the M_n and M_w of the copolymers were obtained using the Mark-Houwink constants for linear polyethene and no correction for methyl side branches was applied. P_n values were then estimated by dividing the obtained M_n values by 28 (molar mass of the monomeric ethene unit). GPC was performed with a Polymer Laboratories PL-220 with Viscotek 220R viscosimeter. Conventional results are calculated with the Mark-Houwink constants of linear PP ($\log K = -3.721$) for the PP samples, and linear PE ($\log K = -3.391$) for the PE/EPR samples.

2.5. ^{13}C-NMR measurements

Ethene and propene contents in the copolymers were determined by ^{13}C-NMR in $C_2D_2Cl_4$. Solution ^{13}C NMR spectra were recorded at 373 K using a Bruker ARX-400 NMR spectrometer and analyzed by standard methods.

3. Computational details

Density functional calculations were performed with the TURBOMOLE program [7] in combination with the OPTIMIZE routine of Baker [8]. As will be justified in Section 4, all calculations used a 2-methylbutyl chain as a model for the growing polymer chain. The ligands were included without simplification. Solvent and counterion effects were ignored. For each system (see Fig. 1), all relevant minima and transition states were fully optimized at the b3-lyp level [9] employing the standard SV(P) basis sets [10] and a small-core pseudopotential for Zr [11]. For starting the transition state optimizations, initial Hessians were computed using the PM3(tm) method as available in the Spartan Pro package of Wavefunction Inc. [12] For the Ind system, possible conformations resulting from C–C rotations of the alkyl chain model were systematically investigated. The most stable conformations were then employed as a starting point for the minimum and transition state computations of substituted catalysts. After optimization, the b3-lyp/SV(P) structures were used for performing b3-lyp single point calculations employing the much larger TZVP basis sets [10,13] and the transition states were subjected to an analytical b3-lyp/SV(P) frequency calculation. As required for a first order saddle point, for each of the computed transition states only one imaginary frequency was obtained. Effective activation energies for H transfer reactions were calculated from the activation free energies (including all thermal corrections) by adding a contribution due to tunneling using the Wigner correction [14]. Overlap populations were computed using Mulliken population analysis.

4. Results and discussion

4.1. Polymerization results

4.1.1. Degree of polymerization P_n

Fig. 2 shows the polymerization degrees (P_n) of the polymers as a function of the mole fraction of propene in the copolymer.

The highest P_n values for both homo- and copolymers are obtained by the simultaneous introduction of the 2-Me substituents and the Benzo or 4-Ph groups. It is clear, however, that these groups have a significantly larger impact on the polymerization degrees of the homopolymers than on those of the copolymers (see below). As has been observed previously [3,4,6,15] especially in the case of propene homopolymerization, the combination of the 4-Ph or Benzo groups with the 2-Me groups turns out to be very effective. Further, in agreement with literature data, P_n of the PP homopolymer is also significantly increased by the introduction of the 2-Me groups alone [4,6,16] whereas the 4-Ph or Benzo systems produce PP with a P_n similar to that of the unsubstituted catalyst. The effect of the 2-Me group has been attributed to the fact that this group suppresses the chain transfer to

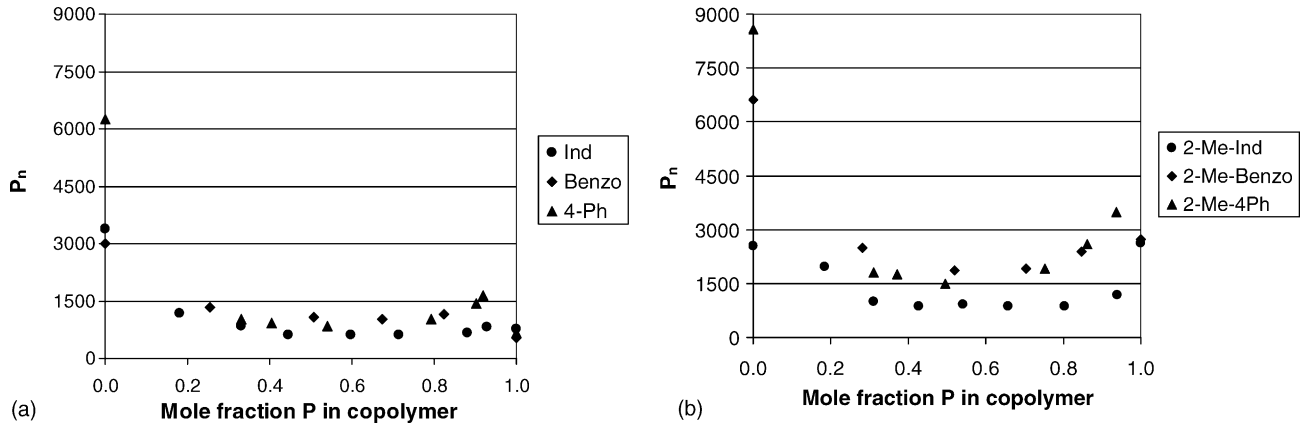

Fig. 2. Experimental degrees of polymerization P_n in E/P copolymerizations for the catalysts of Fig. 1. For the 2-Me-4-Ph variant, P_n for propene homopolymerization is not shown for clarity but is equal to 13095.

propene [6,17]. At least in part, this has been related to a much higher regiospecificity induced by the 2-Me group. As noted by Brintzinger and co-workers, the performance of α-methyl substituted catalysts approaches that of heterogeneous Ziegler catalysts, in which regio-irregularities are not observed [18]. Besides this indirect effect, a direct influence of the 2-Me substituent on slowing down the kinetics of chain transfer to propene has been suggested [4,6,17]. Both from literature data [4] and from Fig. 2, the various substituents appear to have a much lower effect on the polymerization degree of polyethene. According to the data of Fig. 2, even the simultaneous introduction of the Benzo or 4-Ph groups and the 2-Me substituents leads to a maximum increase in P_n by only a factor of ≈2.5 as compared to ≈17 for PP.

4.1.2. Homopolymerization versus copolymerization

For the copolymers (in the range 0.2–0.9 mole fraction propene), the introduction of substituents leads to a maximum change in P_n by a factor of ≈3. The P_n values obtained with the 2-Me-Benzo and 2-Me-4-Ph variants are similar whereas in homopolymerizations the latter catalyst generally performs better. All catalysts produce copolymers with significantly lower P_n than PE homopolymers. Especially for the 4-Ph, 2-Me-4-Ph and 2-Me-Benzo a significant drop in P_n on adding a small amount of propene can be observed. Starting from the PP side on the other hand, a significant drop in P_n is found only for the catalysts bearing 2-Me substituents, as observed previously by Rieger and co-workers [19]. In case of the Benzo and 4-Ph variant the addition of a small amount of ethene leads to copolymers with an even higher degree of polymerization than the PP homopolymers. This suggests the presence of dormant sites in the PP homopolymerizations due to regio-errors in propene insertion, which are being "reactivated" by ethene in the copolymerizations (see further below) but which in the absence of ethene are likely to remain in the dormant state [20].

4.1.3. Comonomer affinities

When describing copolymerization statistics, the reactivity of the different monomers is usually described by means of the copolymerization parameters. Using first-order Markov statistics [21] only two such parameters are employed. These are commonly denoted as r_1 and r_2 and are defined as

$$r_1 = \frac{k_{p,ee}}{k_{p,ep}} \quad r_2 = \frac{k_{p,pp}}{k_{p,pe}} \tag{1}$$

In this notation, each of the k's refers to a specific propagation (as indicated by the first p- subscript) rate constant. The two other subscripts refer to the last inserted monomer in the growing polymer chain and the monomer being inserted, respectively. For example, $k_{p,ep}$ is the rate constant for insertion of propene after ethene. The indices r_1 and r_2 thus denote the preference for ethene or propene homopolymerization over copolymerization. They can be calculated from the applied [P]/[E] ratio in the reactor and the copolymer composition as determined via ^{13}C-NMR. In the current work, the r-values have been obtained following the method of Kakugo [22] using data for mole fractions of E and P in the copolymer in the range of 0.2–0.8. The results (see Table 1) indicate the copolymerization behaviour of the different catalysts to be governed mainly by the substituents on the C_6 ring of the indenyl moiety and only very little by the 2-Me substituents

Table 1
Copolymerization parameters r_1 and r_2 at 50 °C as obtained via the method of Kakugo [21] using first order Markovian statistics

Catalyst	r_1	r_2	$r_1 \times r_2$
Ind	5.36 [0.40]	0.08 [0.02]	0.43
2-Me-Ind	5.39 [0.48]	0.05 [0.01]	0.27
Benzo	4.54 [0.47]	0.29 [0.08]	1.32
2-Me-Benzo	4.48 [0.33]	0.35 [0.07]	1.57
4-Ph	1.84 [0.15]	0.98 [0.11]	1.80
2-Me-4-Ph	2.02 [0.27]	0.88 [0.10]	1.78

Values between square brackets refer to the standard deviations calculated as $[1/(N-1)\Sigma(r_{exp} - r_{mean})^2]^{1/2}$.

in accord with previous observations by Busico et al. [23]. They also show the preference for ethene with respect to propene to decrease in the order (2-Me)-Ind > (2-Me)-Benzo > (2-Me)-4-Ph and denote a much higher dependency of this preference on the last inserted monomer for the Ind and 2-Me-Ind than for the other catalysts. The low r_1 value of the 4-Ph and 2-Me-4-Ph catalysts indicates their relatively low preference for ethene homopolymerization. The r_2 values of these systems show that after a propene insertion the rate constants for ethene and propene propagation are similar. This is remarkable since calculations invariably predict the barrier for ethene insertion to be lower than that of propene insertion in agreement with all other copolymerization parameters ($r_1 > 1$, $r_2 < 1$). It may indicate that the propagation rate constants (especially for the propagation of ethene) are not always determined by the insertion step itself but by, e.g. uptake of the monomer as found previously for the $[(CpSiMe_2NR)TiMe]^+$ system in the presence of the $MeB(C_6F_5)_3^-$ ion [24] or chain rearrangements (see further below). Note however that Busico and co-workers published a somewhat higher r_1 and a somewhat lower r_2 value for the 2-Me-4Ph catalyst of 2.5 and 0.6, respectively [23].

4.1.4. Chain transfer reactions

Several chain transfer reactions can be envisaged:

- Chain transfer to aluminium
- β-Hydrogen transfer to the metal
- β-Hydrogen transfer to the monomer (which in the case of E/P copolymerizations may involve either ethene or propene)

Chain transfer to aluminium is not uncommon when using MAO as a co-catalyst [25]. To investigate if this transfer also occurs in our systems, a series of polymerization experiments using different Al/Zr ratios was performed using the Ind catalyst. Measured activities and P_n values (Supplementary data, Fig. S1) do not show a clear dependence of P_n on the Al/Zr ratio, indicating that—at least for this system—chain transfer to Al is not dominant in E/P copolymerizations. Further information about the predominant transfer reaction was obtained from end-group analysis using ^{1}H NMR. β-Hydrogen transfer results in unsaturated end groups whereas transfer to aluminium eventually results in saturated end groups. After β-hydrogen transfer, vinyl end groups are obtained if the last-inserted unit was ethene, 2-propenyl end groups if it was propene. For the 2-Me-4-Ph catalyst, the unsaturated end groups were mainly 2-propenyl groups, consistent with dominant β-hydrogen transfer after propene insertion. In addition, the amount of unsaturated groups was found to correspond to about one unsaturation per polymer (see Fig. 3).

These results confirm that the predominant transfer reaction does not correspond to transfer to aluminium, but they do not allow discrimination between β-hydrogen transfer to the monomer or to the metal. However, the latter variation would be inconsistent with the observed dependence of molecular weight on ethene concentration [26]. Also, in the literature transfer to the metal is described as energetically unfavourable [27]. As shown by Brintzinger and co-workers, the β-agostic interaction required for such a transfer places the polymer chain of a stereoregular unit into that ligand sector which is occupied by the β-substituent on the Cp ring, i.e. the Indenyl aryl group for the systems of Fig. 1 [18]. It can consequently be concluded that for the metallocenes investigated here, the predominant termination reaction during E/P copolymerizations involves β-hydrogen transfer to the monomer after a propene insertion.

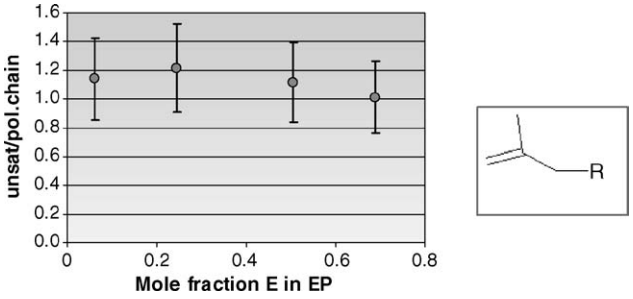

Fig. 3. Unsaturated end groups in E/P copolymers made with the 2-Me-4-Ph catalyst.

4.2. Modeling the molecular weight behaviour in copolymerization: a comparison of theory and experiment

Obviously, when trying to understand trends in molecular weight, one should start from the fundamental equation for P_n. The average degree of polymerization is defined as the number of monomer units per polymer chain and is thus proportional to the ratio of the total rate of all possible propagation reactions (ΣR_p) to the total rate of all possible termination reactions (ΣR_t).

$$P_n = \frac{\Sigma R_p}{\Sigma R_t} \tag{2}$$

Assuming dominant termination via transfer to monomer after propene insertion (see previous section) and first-order Markov statistics [21] the equation becomes

$$P_n = \frac{R_{p,ee} + R_{p,pe} + R_{p,ep} + R_{p,pp}}{R_{t,pe} + R_{t,pp}} \tag{3}$$

with the additional subscripts ee, pe, ep and pp having the same meaning as in Eq. (1).

4.2.1. Expressing P_n in terms of ethene propagation

Assuming no continuous accumulation of E and P terminated growing chains [28], we have $k_{p,pe}$[Zr-P-R][E] = $k_{p,ep}$[Zr-E-R][P] with R the growing chain, and Eq.

(3) can be transformed to

$$P_n = \frac{1}{k_{t,pe}/k_{p,pe} + (k_{t,pp}/k_{p,pe})([P]/[E])} \times \left\{ \frac{[E]}{[P]} r_1 + \frac{[P]}{[E]} r_2 + 2 \right\} \quad (4)$$

with r_1 and r_2 denoting the copolymerization parameters (see Table 1 and Eq. (1)), the k's corresponding to the rate constants of the relevant propagation and termination reactions and [E]/[P] referring to the ethene/propene concentrations in the solvent. This equation can also be written as

$$P_n = \frac{1}{e^{-\Delta G(t,pe-p,pe)/RT} + e^{-\Delta G(t,pp-p,pe)/RT}[P]/[E]} \times \left\{ \frac{[E]}{[P]} r_1 + \frac{[P]}{[E]} r_2 + 2 \right\} \quad (5)$$

with the free activation energy differences ΔG(t, pe − p, pe) and ΔG(t, pp − p, pe) corresponding to transfer to ethene or propene, both relative to insertion of ethene after propene. For each of the investigated catalysts, these free energy differences have been determined by fitting the experimental P_n data to Eq. (5) for a set of data corresponding to different [E]/[P] ratios using the experimental r_1 and r_2 parameters from Table 1. The results of these fittings are shown in Table 2 and depicted as a function of the mol% P in the polymer in Fig. 4.

Note that the P_n values for homopolymerization of ethene and propene were not used in the fit. For ethene homopolymerization, the relevant termination mechanism is not included in the model and Eq. (5) would always yield an infinite P_n. For propene homopolymerization, the differences between the calculated and observed P_n in Fig. 4 show that the main termination reaction differs from that of the copolymerization reactions, thus implying that the assumptions behind (3) do not hold for propene homopolymerization.

In all cases, reasonable fits are obtained. The differences ΔG(t, pp − t, pe) = ΔG(t, pp − p, pe) − ΔG(t, pe − p, pe) indicate a significantly higher free energy barrier (7–12 kJ/mol) for transfer to propene than for transfer to ethene, as expected. They become slightly larger as a result of 2-Me substitution, e.g. 12.3 kJ/mol for 2-Me-Ind versus 10.8 kJ/mol for Ind. In contrast, the introduction of the 4-Ph or Benzo groups is found to reduce the preference for termination to ethene as compared to the Ind catalyst. Inspection of the ΔG(t, pe − p, pe) and ΔG(t, pp − p, pe) columns shows these ΔG(t, pp − t, pe) trends to be determined mainly or even exclusively by a more difficult (in case of the 2-Me substituents) or easier (in case of the Benzo and 4-Ph groups) transfer to propene with respect to ethene insertion. In agreement with the available literature data, the fit results of Table 2 thus indicate that the 2-Me substituent suppresses the transfer to propene (see also in Section 4.1) [6,17].

Table 2 also provides the free energy differences as obtained from density functional calculations at the b3-lyp/TZVP//SV(P) level [29]. The calculations agree with experiment in predicting a much higher free energy barrier for the transfer to propene than to ethene, although the magnitude of this preference is clearly overestimated (see also Fig. 5c): the calculations predict $k_{t,pe}/k_{t,pp}$ values of 2–45 × 10^3, while the fit results are about 200 times smaller (in the range of ca. 10–100).

Further in accordance with the fit results, the calculations predict an increase of ΔG(t, pe − p, pe) and ΔG(t, pp − p, pe) on introducing the 2-Me substituents (see also Fig. 5a and b) and for both the Ind and 4-Ph variant they indicate the ΔG(t, pp − t, pe) to be affected mainly by the transfer to propene. However, the calculations do not always correctly predict the effect of the Benzo and 4-Ph groups, e.g. whereas the fitted ΔG(t, pp − p, pe) show a clear decrease on introducing either of these groups, the calculated ΔG(t, pp − p, pe) increase. Also, similarly to the activation free energy differences between the two termination reactions, the calculated free energy differences between propagation and termination are systematically too large, leading to strongly overestimated P_n values. Even the trends of these latter free energy differences are not correctly reproduced, as is clear from the scatter in Fig. 5a and b.

Various reasons for this discrepancy between theory and experiment may be envisaged:

A. Neglect of solvent and anion effects:

A1: The solvent and/or anion may have an effect that depends strongly on ligand structure, thus destroying any trends that would exist in the gas phase.

A2: The rate-determining step may have shifted from olefin insertion to olefin capture due to solvent/anion effects, possibly only in some cases [24,30].

Table 2
Activation free energy differences ΔG(t, pe − p, pe), ΔG(t, pp − p, pe) and ΔG(t, pp − t, pe) (kJ/mol) as obtained by fitting the fitting the experimental P_n data (see Fig. 2) to Eq. (5) and from density functional calculations at the b3-lyp/TZVP//SV(P) level

Catalyst	ΔG(t, pe − p, pe)		ΔG(t, pp − p, pe)		ΔG(t, pp − t, pe)	
	Fit	Calculated	Fit	Calculated	Fit	Calculated
Ind	14.4	25.4	25.1	49.7	10.8	24.3
2-Me-Ind	15.3	25.9	27.6	52.1	12.3	26.2
Benzo	15.2	27.5	23.6	56.3	8.4	28.8
2-Me-Benzo	16.4	32.9	26.2	58.2	9.7	25.3
4-Ph	14.4	33.6	21.3	54.6	6.9	21.0
2-Me-4-Ph	15.9	36.4	25.8	61.8	9.9	25.4

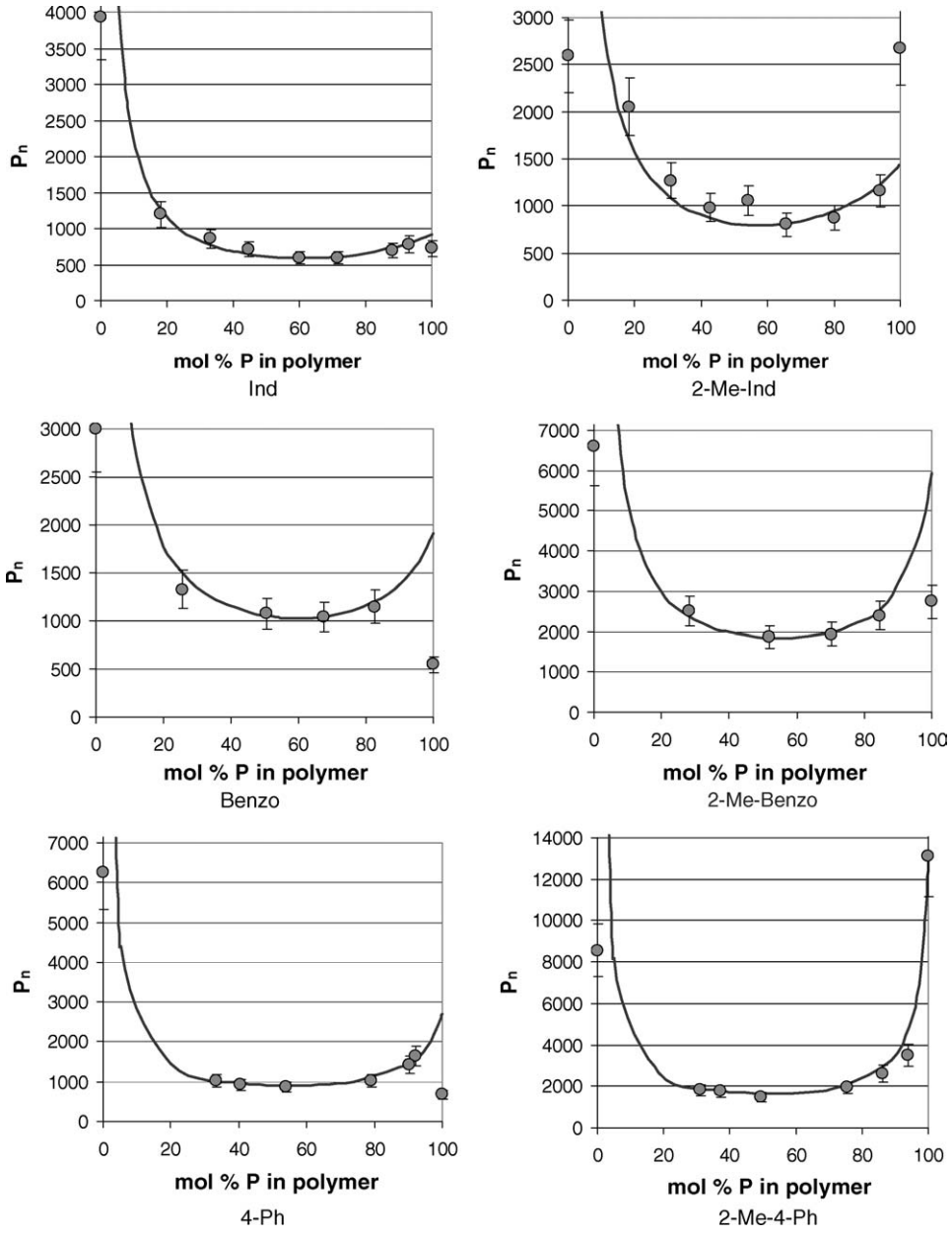

Fig. 4. Fit results.

B. Contribution of additional termination reactions.
C. Failure of the b3-lyp/TZVP//SV(P) method.
D. The rate-determining step of olefin (especially ethene) propagation does not correspond to the insertion of ethene but e.g. to a rotation of the growing alkyl chain [31].

For the series of very similar catalyst structures investigated here, solvent and anion effects are not very likely to affect trends (possibility A1). Possibility A2 cannot be excluded at present. Recent literature data has revealed that the solvent and/or anion may indeed alter the rate-determining step for chain propagation from insertion to uptake (see e.g. 24). However, for the complex systems investigated here we have no way of checking this. In the density functional studies on Zirconocene-MAO systems that have been published thus far, various model systems for the MAO cocatalyst have been employed as the structure of MAO is not precisely known [32]. We have not been able to come up with any plausible alternative termination mechanisms that are consistent with the experimental observations (possibility B) [33]. Concerning the accuracy of the b3-lyp/TZVP//SV(P) method (possibility C), it has been shown previously that hybrid functionals like b3-lyp lead to differences between termination and propagation deviating at most 1 kcal/mol from extrapolated CCSD(T) values whereas the pure functionals underestimate this difference by 3–4 kcal/mol [27]. In combination with the relatively large

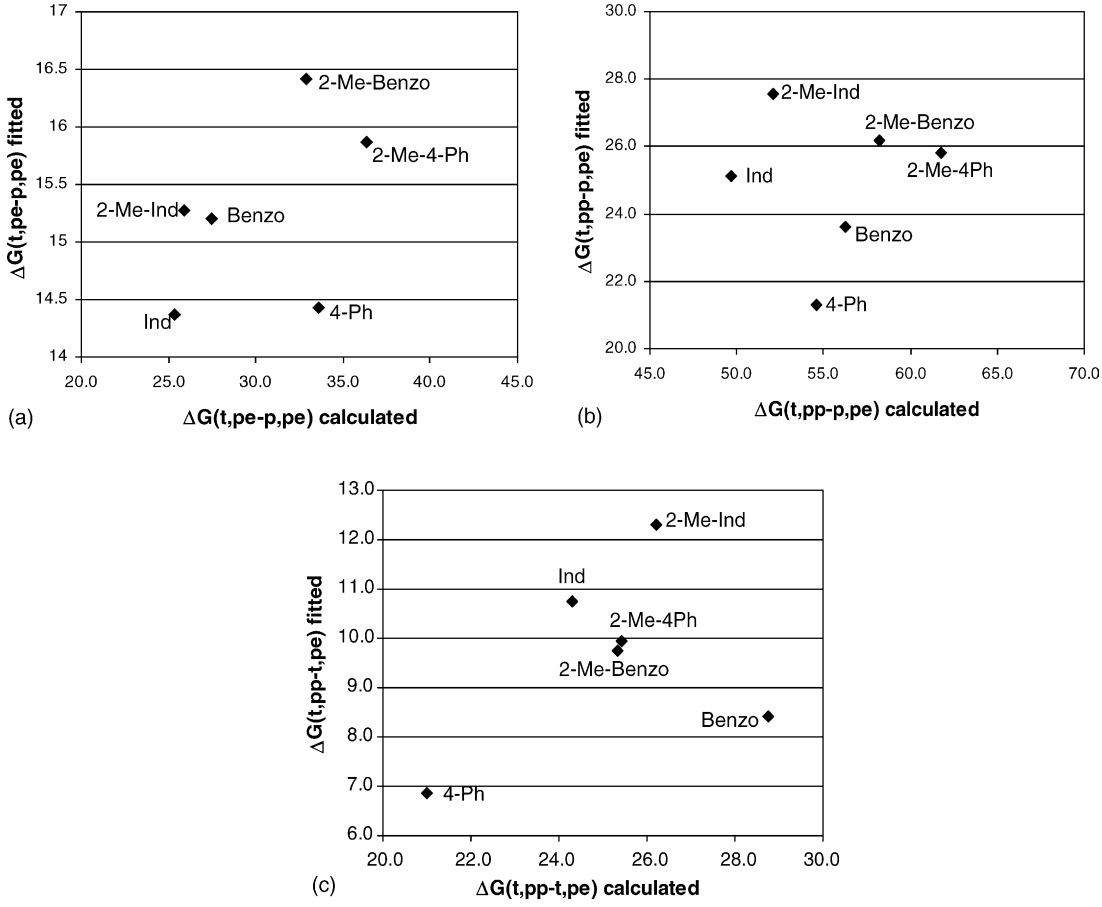

Fig. 5. Fitted ΔG values based on Eq. (5) versus calculated values at the b3-lyp/TZVP//SV(P) level (kJ/mol).

TZVP basis sets, it may thus be expected that our method of choice is sufficiently accurate for our purpose [34].

Let us now turn to the possibility (D) that the rate-determining step of ethene propagation does not correspond to the insertion step but to a rotation of the growing chain. Fig. 6 indicates how this may be the case.

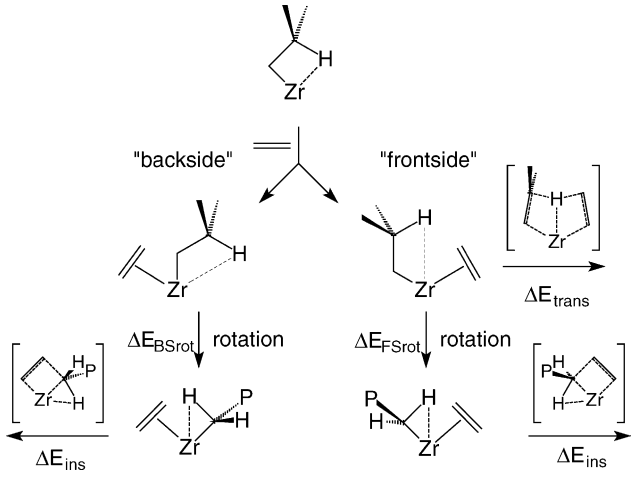

Fig. 6. The possible effect of chain rotation on the propagation of ethene.

Whereas H-transfer can occur directly from the olefin complex in the frontside approach, ethene insertion requires the growing polymer chain to undergo rearrangements before this reaction can take place. Different rotations for frontside and backside attack are required. Frontside rotation basically implies the breaking of the β-agostic interaction and is characterized by a TS having a geometry close to the H-transfer TS. Backside rotation on the other hand is more or less a rotation around the C_α–C_β bond and involves a TS with vicinal interactions. In contrast to solvent and counterion effects, these rotations can be evaluated theoretically in a straightforward manner on the isolated gas-phase cationic olefin complexes by performing constrained optimizations for various Si–Zr–C_α–C_β values. The resulting b3-lyp/SV(P) energy profiles for rotation around the Zr–C_α bond of the Ind and 2-Me-4-Ph systems are shown in Fig. 7. In these curves, the fully optimized “frontside” ethene complex has been taken as a reference.

The profiles are not smooth, due to a strong coupling of the Zr–C_α rotation with the C_α–C_β rotation: as a result of steric hindrance the change from Si–Zr–C_α–C_β = 60 to 75° is accompanied by an abrupt change of the Zr–C_α–C_β–C_γ(ethyl) angle. Fig. 7 also includes the transition states for the two types of rotation and for the insertion

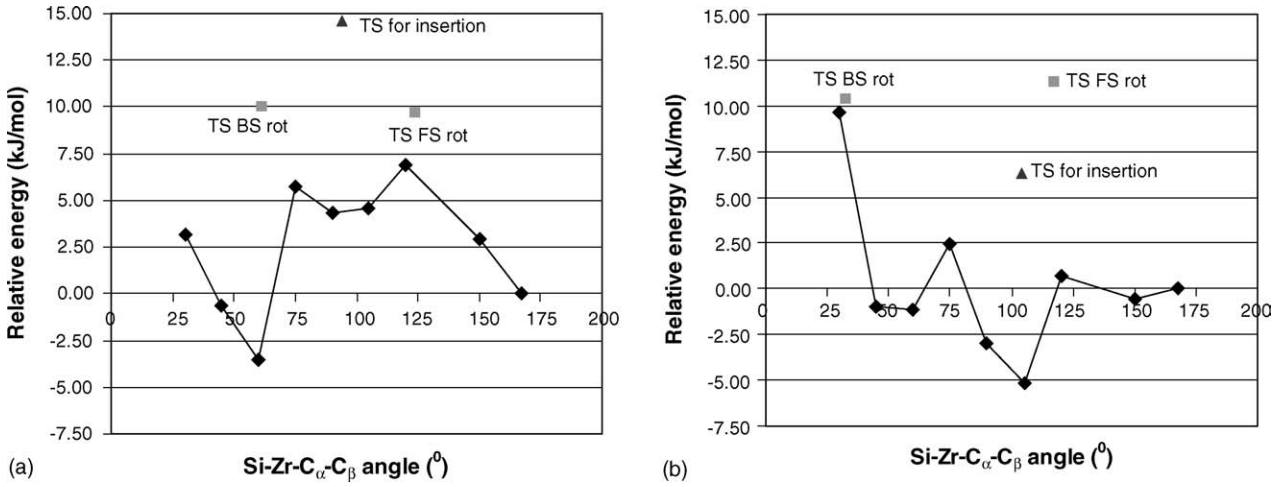

Fig. 7. b3-lyp/SV(P) energy profiles for the Ind (left) and 2-Me-4-Ph (right) as a function of the Si–Zr–C_α–C_β angle.

step. For the Ind system, the rate-limiting step of ethene propagation appears to be the insertion step. On the other hand, the 2-Me-4-Ph variant has a much more corrugated rotation profile, in which several points are above the insertion TS. Here, rotation may well be rate limiting. Similar calculations employing the BP86 functional (which tends to produce lower insertion barriers) indicate a higher barrier for rotation than for the insertion step for both catalysts. It can thus be concluded that the rotation of the growing alkyl chain may indeed be important. Unfortunately however, finding all relevant transition states for chain rearrangements is far from trivial. Also, as already recognized in the above, solvent and anion effects may be important as well.

4.2.2. Expressing P_n in terms of propene propagation

As propene insertion is characterized by a higher barrier than ethene insertion, this insertion is likely to be the rate-limiting step of the propene propagation for all catalysts investigated. To avoid including chain rotation explicitly in our model, we therefore decided to rewrite Eqs. (4) and (5) in terms of propene propagation. Using the definition for r_2 (see equation (1)) Eq. (4) can be rewritten as:

$$P_\mathrm{n} = \frac{1/r_2}{k_{\mathrm{t,pe}}/k_{\mathrm{p,pp}} + (k_{\mathrm{t,pp}}/k_{\mathrm{p,pp}})([\mathrm{P}]/[\mathrm{E}])} \times \left\{ \frac{[\mathrm{E}]}{[\mathrm{P}]} r_1 + \frac{[\mathrm{P}]}{[\mathrm{E}]} r_2 + 2 \right\} \quad (6)$$

or in terms of the corresponding free energy changes

$$P_\mathrm{n} = \frac{1/r_2}{\mathrm{e}^{-\Delta G(\mathrm{t,pe-p,pp})/RT} + \mathrm{e}^{-\Delta G(\mathrm{t,pp-p,pp})/RT}[\mathrm{P}]/[\mathrm{E}]} \times \left\{ \frac{[\mathrm{E}]}{[\mathrm{P}]} r_1 + \frac{[\mathrm{P}]}{[\mathrm{E}]} r_2 + 2 \right\} \quad (7)$$

In combination with the copolymerization parameters from Table 1, fitting the experimental P_n data for different [E]/[P] ratios to Eq. (7) thus provides the free energy differences ΔG(t, pe − p, pp) and ΔG(t, pp − p, pp) (Table 3).

Note that the ΔG(t, pp − t, pe) values obtained from these fits deviate at most 0.4 kJ/mol from those in Table 2, thereby giving confidence in our fit results. In contrast, considering the free energy differences with respect to propagation, the data in Table 3 (propene reference) reveal some significant differences with those of Table 2 (ethene reference). Whereas the previously discussed ΔG(t, pp − p, pe) decrease when introducing the 4-Ph or Benzo substituents, the ΔG(t, pp − p, pp) increase. Also, the ΔG(t, pe − p, pp) are significantly more affected by the 4-Ph and Benzo groups than the ΔG(t, pe − p, pe). Note that for the two 4-Ph variants the ΔG with respect to the propagation of ethene and propene are identical whereas for all other catalysts both the ΔG(t, pe − p, pp) and ΔG(t, pp − p, pp) are smaller than the ΔG analogues with respect to ethene propagation, in perfect agreement with the (experimental) r_2 parameters. Gratifyingly, the propene-referenced ΔG lead to a better correlation between theory and experiment (Fig. 8) than the ethene-referenced data of Fig. 5.

We take this as an indication that of the four reactions studied (ethene and propene propagation and termination) only one, namely ethene propagation is “anomalous”. The ΔG(t, pp − p, pp) values are calculated too high with deviations between theory and experiment between ca. 5–11 kJ/mol. As far as the ΔG(t, pe − p, pp) values are concerned, two groups can be distinguished: one for the catalysts without the 2-Me groups and one for the catalysts with the 2-Me groups. Whereas for the latter set, the computed ΔG are at most 5.7 kJ/mol smaller than the fitted ones, for the catalysts not containing the 2-Me groups the computed ΔG(t, pe − p, pp) are systematically too small by 8.7–10.4 kJ/mol. Interestingly, these two catalyst groups also showed different trends in P_n on going from the PP homopolymer to the E/P copolymer. For the catalysts with the 2-Me groups, adding a small amount of ethene leads to a drop in P_n, whereas for those without the 2-Me groups an increase in P_n was observed (see

Table 3
Activation free energy differences ΔG(t, pe − p, pp), ΔG(t, pp − p, pp) and ΔG(t, pp − t, pe) (kJ/mol) as obtained by fitting the fitting the experimental P_n data (see Fig. 2) to Eq. (7) and from density functional calculations at the b3-lyp/TZVP//SV(P) level

Catalyst	ΔG(t, pe − p, pp)		ΔG(t, pp − p, pp)		ΔG(t, pp − t, pe)	
	Fit	Calculated	Fit	Calculated	Fit	Calculated
Ind	7.7	−1.0	18.3	23.3	10.8	24.3
2-Me-Ind	7.5	2.7	19.6	28.9	12.1	26.2
Benzo	11.9	1.5	20.3	30.2	8.5	28.8
2-Me-Benzo	13.7	8.0	22.9	33.3	9.3	25.3
4-Ph	14.4	5.1	21.3	26.1	6.8	21.0
2-Me-4-Ph	15.5	11.2	25.7	36.6	10.2	25.4

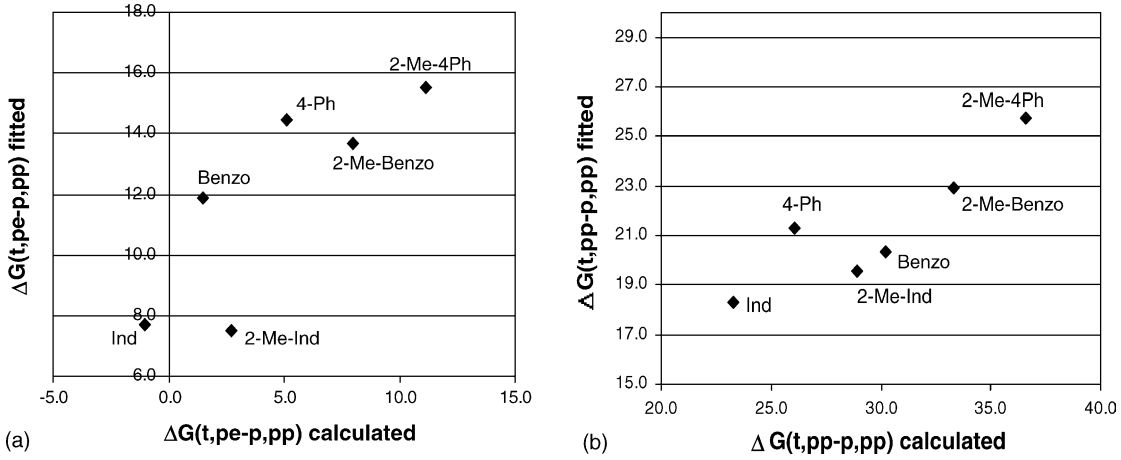

Fig. 8. Fitted ΔG values based on Eq. (8) and the r_2 values of Table 2 versus calculated values at the b3-lyp/TZVP//SV(P) level (kJ/mol).

Fig. 4), attributed here to a reactivation of the dormant sites in the PP polymers [35].

4.2.3. r_2 values

The theoretical P_n prediction described earlier required us to compute the kinetics of both ethene and propene insertion. If these insertion reactions were the rate-limiting steps for ethene and propene propagation it would be possible to predict the r_2 values (see Eq. (1)) from the calculations. We have seen however that for the ethene monomer this assumption may not be valid, so even in a qualitative sense, no good agreement between the theoretical and experimental r_2 values can be expected. Plotting these values against each other (see Fig. 9) indeed reveals that the computations are not even able to reproduce the experimental trends.

In fact, the reason that the transformation in (7) produces acceptable agreement between theory and experiment is that all anomalies related to ethene insertion are put into r_2.

4.3. Propene homopolymerization

Whereas the various substituents hardly affect the molecular weights of the E/P copolymers, we have seen previously in Section 4.1 that the simultaneous introduction of the 2-Me and 4-Ph or Benzo groups has a significant impact on the molecular weights of the propene homopolymers. Under the assumption that the dominant termination reaction during propene homopolymerization is H-transfer to propene, the degree of polymerization P_n of the PP homopolymers is simply given by

$$P_n = e^{\Delta G(t,pp\text{-}p,pp)/RT} \quad (8)$$

with ΔG(t, pp − p, pp) having the same definition as in Eq. (7). It is tempting to predict the P_n data of the PP

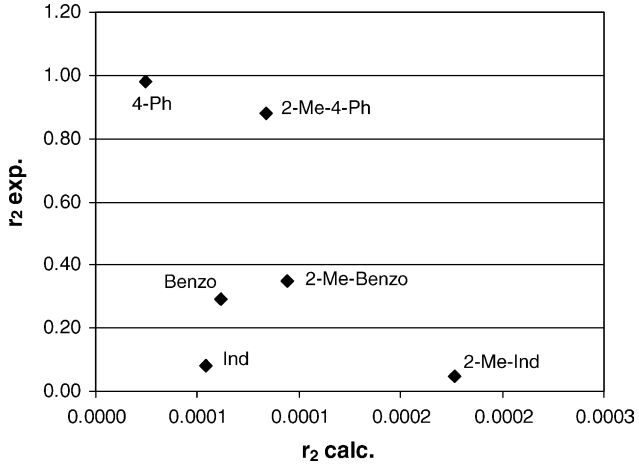

Fig. 9. Calculated versus experimental (see Table 1) r_2 values of the catalysts of Fig. 1.

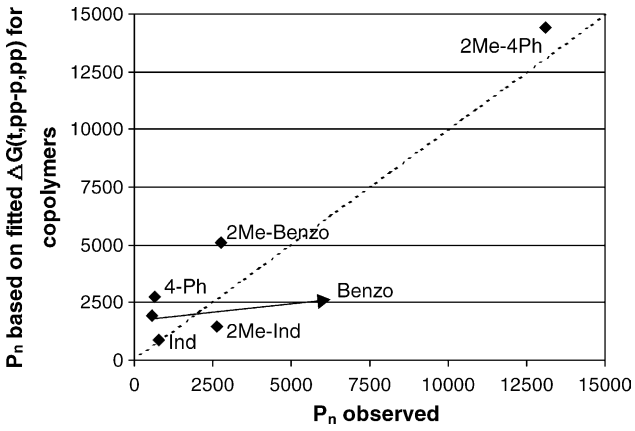

Fig. 10. Predicted P_n based on Eq. (9) and the ΔG(t, pp − p, pp) based on the copolymerization data versus observed P_n for PP homopolymers.

homopolymers using the ΔG(t, pp − p, pp) values that have been obtained based on the P_n results of the copolymers (see the results in Table 3). These predictions are compared with the observed P_n for the homopolymers in Fig. 10.

It can be seen that, except for the 2-Me-Ind, the predicted P_n based on the ΔG(t, pp − p, pp) fitted to the copolymerization results are higher than the P_n values being observed experimentally for the homopolymers. Based on the computed ΔG(t, pp − p, pp) the predicted P_n are even larger. These differences between predicted and observed P_n must be ascribed to the contribution of alternative chain termination mechanisms during homopolymerization such as, e.g. transfer to Al and/or differences in regio-selectivity [18], which we assumed to be negligible in copolymerizations. It thus seems that it is possible to learn more about propene homopolymerization by studying E/P copolymerization, i.e. the ΔG(t, pp − p, pp) of Table 3 can be considered to be more representative for the free energy differences between the H-transfer to and propagation of propene than those that could be derived from Eq. (8) using the P_n results of the PP homopolymers.

4.4. A rationalization for the trends in ΔG

4.4.1. Contributions to ΔG

In order to get a better understanding of the trends in the computed ΔG values at 323 K, let us now analyze in more detail the various contributions to each of these free energy differences. These involve:

- The b3-lyp/SV(P) total energy differences ΔE.
- The zero-point energy differences ΔZPE.
- The pV term, which cancels in all comparisons.
- The thermal enthalpy correction $\Delta H(0) \rightarrow \Delta H(323)$.
- The entropy contribution −TΔS(323).
- The Wigner contributions ΔWigner (tunneling effects), obtained here by converting the rate contribution factor to an effective energy contribution.

Thus, $\Delta G(323)$ can be written as:

$$\begin{aligned}\Delta G(323) &= \Delta E + \Delta\mathrm{ZPE} + \Delta(\Delta H(0)\\ &\rightarrow \Delta H(323)) - T\Delta S(323) + \Delta\mathrm{Wigner}\\ &= \Delta H(0) + \Delta(\Delta H(0)\\ &\rightarrow \Delta H(323)) - T\Delta S(323) + \Delta\mathrm{Wigner}\\ &= \Delta H(323) - T\Delta S(323) + \Delta\mathrm{Wigner}\end{aligned}$$

For each of the $\Delta G(323)$ values discussed previously in Sections 4.2 and 4.3, the above-mentioned contributions are plotted versus the total $\Delta G(323)$ in Fig. 11.

The ΔG values are dominated by the enthalpies. Thermal contributions to these enthalpies are small, $\Delta H(323)$ being very similar to $\Delta H(0)$. The contributions resulting from the Wigner corrections are small, accounting for a change in $\Delta G(323)$ of up to −2 kJ/mol; their contribution to differences in transfer barriers is negligible. ZPE corrections are significant and favor termination over propagation by up to 10 kJ/mol, but nearly cancel between reactions of the same type. Entropy contributions $|T\Delta S|$ are between ca. 0 and 10 kJ/mol. In case of the ΔG(t, pe − p, pp) and ΔG(t, pp − p, pp) they follow the ΔE trends, for ΔG(t, pp −t, pe) they dominate the variation of ΔG with ligand structure.

4.4.2. Effect of ligand structure on ΔG

Fig. 11c shows that ΔE(t, pp − t, pe) is rather insensitive to ligand structure, staying within the range of 18.4–20.1 kJ/mol for all ligands studied. However, the various energy differences between termination and propagation steps, ΔE(t, xx − p, yy), turn out to be much more dependent on substituent effects. It may be anticipated that especially the transition states for hydrogen transfer will be sensitive to steric substituent effects. These require a six-membered ring with all ring atoms in the same plane, whereas the transition states for insertion require a four-membered metallacyclobutane ring (see e.g. the relevant TS for the Ind system in Fig. 12).

During hydrogen transfer the C_α–C_β rotation becomes frozen out, offering fewer possibilities to the growing chain to avoid the additional substituents than during the insertion process. Also, considerably larger C_{ethene}–Si–C_α angles are required. Hydrogen transfer thus involves more steric hindrance around the metal center than insertion. This is confirmed clearly by CPK models of the various transition states. During hydrogen transfer the 2-Me group is considerably closer to the ethene and the growing chain than during the insertion reaction; also, the growing chain comes closer to or even makes contact with the Benzo or 4-Ph groups if present. Thus, substituent effects on ΔE are plausibly explained by steric interactions. The compression caused by the 2-Me group, in particular, is seen to weaken the interaction between the metal and the migrating β-hydrogen atom in the H transfer transition states, as can be seen from the longer Zr–H_β and shorter C–H_β distances (e.g., 2.059 and

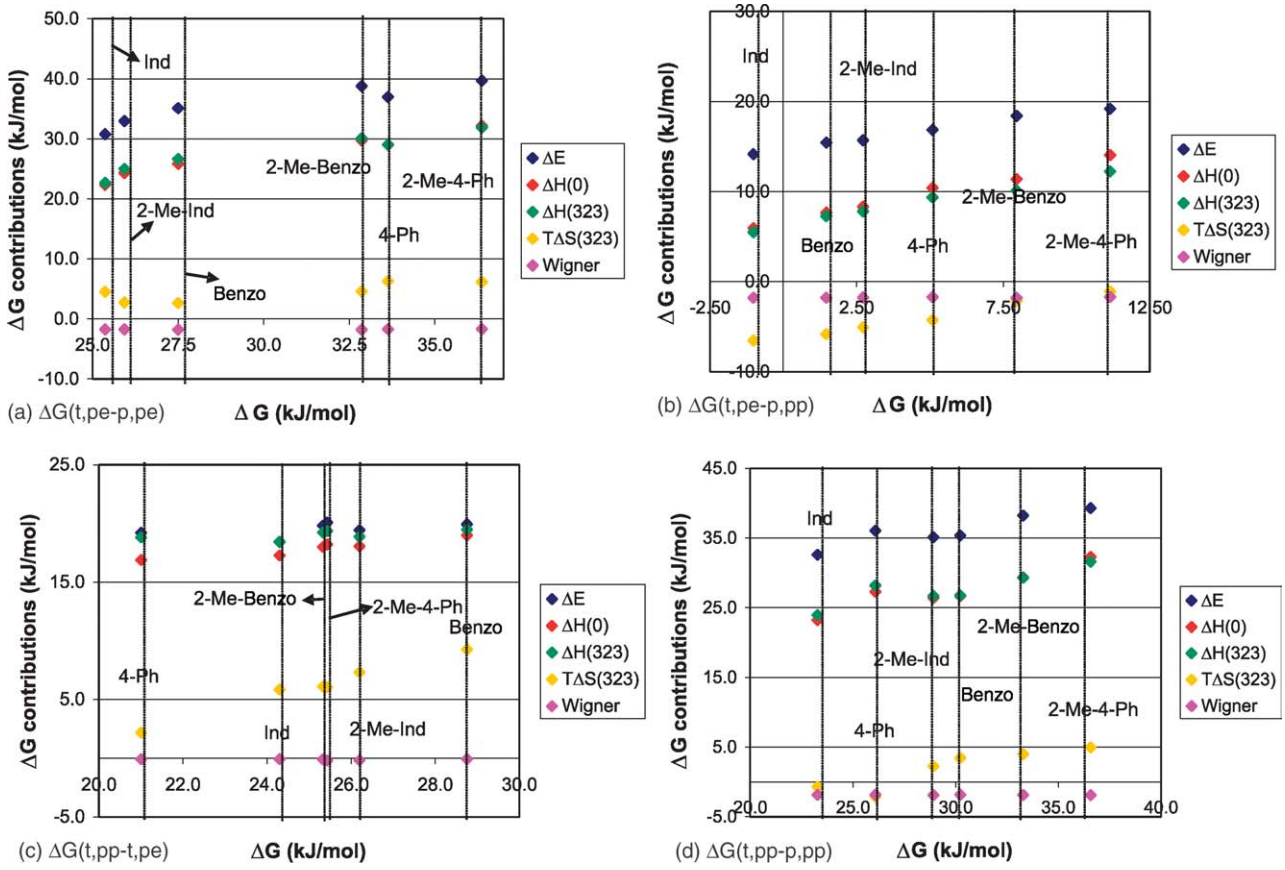

Fig. 11. The various contributions to the calculated ΔG values (kJ/mol).

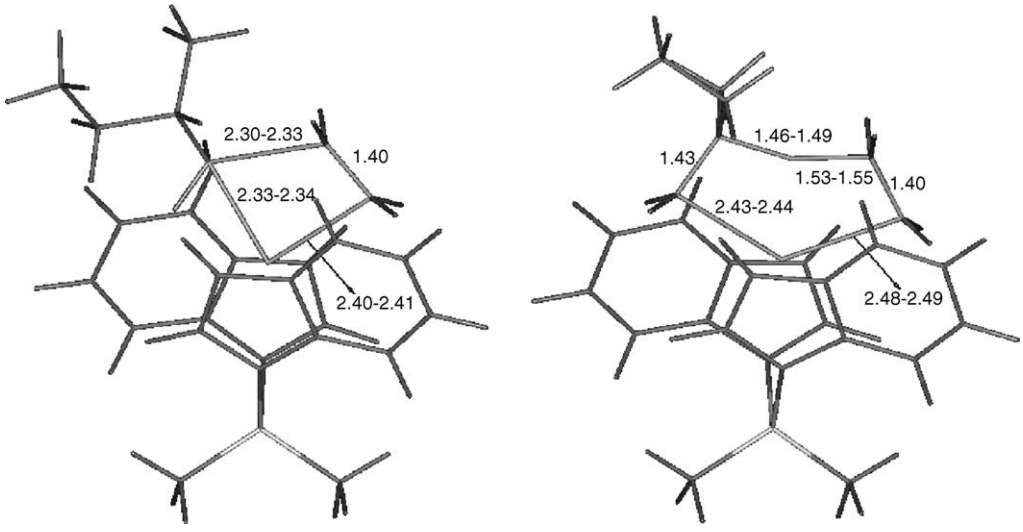

Fig. 12. Transition states for the insertion of (left) and H-transfer (right) to ethene for the Indenyl system with the atoms in orange in a plane and some typical distances in Å.

1.482 Å for Ind; 2.071 and 1.468 Å for 2-Me-Ind). Furthermore, based on a Mulliken population analysis significantly smaller Zr–H_β overlap populations are found for the catalysts with the 2-Me than for those without the 2-Me groups (see supplementary information, Supplementary data, Table S2).

5. Conclusions

Describing trends in molecular weights for ethene/propene copolymerization, using calculated relative free energies for monomer insertion and chain transfer to

monomer, does not work. Our results suggest that this may be due to ethene propagation being limited by a step different from the insertion itself. Besides other possible hypotheses, in particular counterion effects, we have shown that a larger energy barrier may be associated with chain rotation. Combination of experimental r_2 values with calculated barriers for propene propagation and chain transfer to both monomers works much better, presumably because the anomalies associated with ethene insertion are concentrated in this experimental r_2 value. The fair agreement achieved for this mixed description method indicates that for the other reactions the rate-limiting steps are "normal".

Propene homopolymerization also appears to be complicated. The results described here indicate that "dormant" species can be important, and show that studies of *co*polymerization can yield valuable information about homopolymerization.

It appears that preparing high molecular weight copolymers requires catalyst modifications displaying a more balanced ratio of propagation and termination.

Acknowledgments

Geert van der Velden and Harrie Linssen of DSM Research are thanked for the NMR measurements, Wilma Limpens and Sjaar Jacobs of DSM Research are thanked for the GPC measurements.

Appendix A. Supplementary data

Supplementary data associated with this article can be found, in the online version, at doi:10.1016/j.molcata.2005.06.066

References

[1] Eur. Chem. News2003, 10–16 February 2003, p. 12.
[2] E.P. Moore, Polypropylene Handbook, Hanser Publishers, 1996, p. 97.
[3] W. Spaleck, M. Antberg, J. Rohrmann, A. Winter, B. Bachmann, P. Kiprof, J. Behn, W.A. Herrmann, Angew. Chem. Int. Ed. Engl. 31 (1992) 1347.
[4] W. Spaleck, F. Küber, A. Winter, J. Rohrmann, B. Bachmann, M. Antberg, V. Dolle, E.F. Paulus, Organometallics 13 (1994) 954.
[5] D. Fischer, in: Presentation at Metcon 2001, 18 May 2001.
[6] U. Stehling, J. Diebold, R. Kirsten, W. Röll, H.H. Brintzinger, Organometallics 13 (1994) 964.
[7] (a) R. Ahlrichs, M. Bär, M. Häser, H. Horn, C. Kölmel, Chem. Phys. Lett. 162 (1989) 165;
(b) O. Treutler, R. Ahlrichs, J. Chem. Phys. 102 (1995) 346;
(c) R. Ahlrichs, M. Bär, H.-P. Baron, R. Bauernschmitt, S. Böcker, M. Ehrig, K. Eichkorn, S. Elliott, F. Furche, F. Haase, M. Häser, C. Hättig, H. Horn, C. Huber, U. Huniar, M. Kattannek, A. Köhn, C. Kölmel, M. Kollwitz, K. May, C. Ochsenfeld, H. Öhm, A. Schäfer, U. Schneider, O. Treutler, K. Tsereteli, B. Unterreiner, M. von Arnim, F. Weigend, P. Weis, H. Weiss Turbomole Version 5, January 2002, Theoretical Chemistry Group, University of Karlsruhe.
[8] (a) PQS version 2.4, 2001. Parallel Quantum Solutions, Fayetteville, Arkansas, USA (the Baker optimizer is available separately from PQS upon request);
(b) J. Baker, J. Comput. Chem. 7 (1986) 385.
[9] (a) C. Lee, W. Yang, R.G. Parr, Phys. Rev. B 37 (1988) 785;
(b) A.D. Becke, J. Chem. Phys. 98 (1993) 1372;
(c) A.D. Becke, J. Chem. Phys. 98 (1993) 5648;
(d) All calculations were performed using the Turbomole functional "b3-lyp", which is not identical to the Gaussian "B3LYP" functional.
[10] A. Schäfer, H. Horn, R. Ahlrichs, J. Chem. Phys. 97 (1992) 2571.
[11] D. Andrae, U. Haeussermann, M. Dolg, H. Stoll, H. Preuss, Theor. Chim. Acta 77 (1990) 123.
[12] PC Spartan Pro version 1.0.3 January 2000 from Wavefunction Inc. 18401 Von Karman Ave, Suite 370, Ivrine, CA 92612.
[13] A. Schäfer, C. Huber, R. Ahlrichs, J. Chem. Phys. 100 (1994) 5829.
[14] E.P. Wigner, Z. Phys. Chem. (Münich) B19 (1932) 203.
[15] Resconi et al., Chem. Rev. 100 (2000) 1253, references herein.
[16] M. Aulbach, F. Küber, Chemie Unserer Zeit 28 (1994) 197.
[17] L. Cavallo, G. Guerra, Macromolecules 29 (1996) 2729.
[18] W. Röll, H.-H. Brintzinger, B. Rieger, R. Zolk, Angew. Chem. Int. Ed. Engl. 29 (1990) 279.
[19] J. Voegele, C. Troll, B. Rieger, Macromol. Chem. Phys. 203 (2002) 1918.
[20] (a) V. Busico, R. Cipullo, J.C. Chadwick, J.F. Modder, O. Sudmeijer, Macromolecules 27 (1994) 7538;
(b) V. Busico, R. Cipullo, V. Romanelli, S. Ronca, M. Togrou, J. Am. Chem. Soc. 127 (2005) 1608.
[21] It is likely that at least second-order Markov statistics are required for an accurate description of the copolymerization [23]. However, the computational data were all obtained with the same 2-methylbutyl chain model, which implicitly assumes a first-order model.
[22] M. Kakugo, Y. Natito, K. Mizunuma, T. Miyatake, Macromolecules 15 (1982) 1150.
[23] V. Busico, R. Cipullo, A.L. Segre, Macromol. Chem. Phys. 203 (2002) 1403.
[24] Z. Xu, K. Vanka, T. Ziegler, Organometallics 23 (2004) 104.
[25] S. Lieber, H.H. Brintzinger, Macromolecules 33 (2000) 9192.
[26] For copolymers obtained using low mole fractions of ethene, the results should be similar to those in which only [ethene] was varied. The observed lowering of P_n with increasing ethene incorporation, combined with the observation of propenyl end groups, is thus inconsistent with a chain transfer mechanism that does not require ethene.
[27] (a) T.K. Woo, L. Fan, T. Ziegler, Organometallics 13 (1994) 2252;
(b) P. Margl, L. Deng, T. Ziegler, J. Am. Chem. Soc. 121 (1999) 154;
(c) K. Thorshaug, J.A. Støvneng, E. Rytter, M. Ystenes, Macromolecules 31 (1998) 7149;
(d) G. Talarico, A.N.J. Blok, T.K. Woo, L. Cavallo, Organometallics 21 (2002) 4939.
[28] An accumulation of secondary M-polymeryl bonds can occur in PP homopolymerizations (dormant sites). However, for EP copolymerizations, it can be assumed that ethene inserts with very similar rates into primary and secondary M-polymeryl bonds (see 20.b).
[29] Formally, the reference complexes used to calculate activation energies are irrelevant, since - assuming olefin complexation as a rapid pre-equilibrium - their energies cancel when evaluating the $\Delta\Delta G$ values we are interested in. Still, it is convenient to use some kind of "reasonable" reference complex. In the present work, we used the olefin-free cationic alkyl complexes (most of which prefer a β-agostic structure) as references.
[30] G. Lanza, I.L. Fragala, T.J. Marks, Organometallics 21 (2002) 5594.
[31] Ziegler already calculated that for ethene insertion in Cp2ZrEt+ rotation of the ethyl group out of its β-agostic position is rate-limiting. However, that result was obtained with a functional known to overestimate weak (e.g. β-agostic) interactions and suspected to

underestimate olefin insertion barriers: J.C.W. Lohrenz, T.K. Woo, T. Ziegler, J. Am. Chem. Soc. 117 (1995) 12793.

[32] (a) Z. Xu, K. Vanka, T. Firman, A. Michalak, E. Zurek, C. Zhu, T. Ziegler, Organometallics 21 (2002) 2444;
(b) E. Zurek, T. Ziegler, Faraday Discuss. 124 (2003) 93;
(c) P.G. Belelli, M.M. Branda, N.J. Castellani, J. Mol. Catal. A 192 (2003) 9.

[33] Chain termination via H_2 in situ produced by the employed metallocene catalysts can be excluded on the basis of NMR results: see C.S. Christ Jr., J.R. Eyler, D.E. Richardson, J. Am. Chem. Soc. 112 (1990) 596; L. Resconi, J. Mol. Catal. A 146 (1999) 167.

[34] The differences between b3-lyp/SV(P) and b3-lyp/TZVP were very small, indicating that further enhancement of the basis set will not have significant effects.

[35] (a) V. Busico, R. Cipullo, P. Corradini, Macromol. Chem. Rapid Commun. 14 (1993) 97;
(b) T. Tsutsui, N. Kashiwa, A. Mizuno, Macromol. Chem. Rapid Commun. 11 (1990) 565.